Revista Mexicana de Astronomía y Astrofísica, **60**, 403–412 (2024)

https://doi.org/10.22201/ia.01851101p.2024.60.02.18

X-RAY OBSERVATIONS OF THE VERY-FAINT X-RAY TRANSIENT XMMSL1 J171900.4–353217: A NEW CANDIDATE NEUTRON STAR LOW-MASS X-RAY BINARY

O. Ahmed[1,2], N. Degenaar[3], R. Wijnands[3], and M. Armas Padilla[4,5]

Received November 14 2023; accepted August 15 2024

ABSTRACT

XMMSL1 J171900.4–353217 is a very-faint X-ray transient that was discovered in 2010 March when it exhibited an outburst. We report on 7 observations, obtained with the X-Ray Telescope (XRT) aboard the Neil Gehrels *Swift* Observatory between 2010 May and October. By fitting a single absorbed power-law model to the XRT spectra, we infer power-law indices of $\Gamma = 1.8 - 2.7$ and an absorption column density of $N_{\rm H} = (4.6 - 7.9) \times 10^{22}$ cm^{-2}. The inferred $0.5 - 10$ keV luminosity fluctuated irregularly and peaked at $L_{\rm X} \simeq 10^{35} - 10^{36}$ erg s^{-1} for a distance of $4 - 12$ kpc. Based on the evolution of the power-law index with varying luminosity, we propose that the source most likely is a transient neutron star low-mass X-ray binary located at several kpc. If true, it would be a good candidate to search for coherent millisecond pulsations when it enters a new accretion outburst.

RESUMEN

XMMSL1 J171900.4-353217 es una binaria de rayos-X transitoria poco luminosa descubierta en marzo de 2010 durante una erupción. Presentamos 7 observaciones obtenidas entre mayo y octubre de 2010 con el Telescopio de Rayos-X (XRT) a bordo del Observatorio Neil Gehrels Swift. Mediante el ajuste de los espectros del XRT con un modelo de ley de potencias absorbido, obtenemos un índice fotónico de Γ=1.8–2.7 y una densidad de la columna de hidrógeno de $N_{\rm H}$=(4.6–7.9)$\times 10^{22}$cm^{-2}. La luminosidad, en el intervalo $0.5 - 10$ keV, fluctuó irregularmente, con picos de $L_{\rm X} \approx 10^{35} - 10^{36}\,{\rm erg\,s^{-1}}$ para una distancia de $4 - 12\,{\rm kpc}$. Basándonos en la evolución del índice fotónico con la luminosidad, proponemos que la fuente es probablemente una binaria de rayos-X poco masiva con una estrella de neutrones situada a varios kpc. De ser cierto, esta fuente sería una buena candidata para buscar pulsaciones coherentes de milisegundos cuando entre de nuevo en erupción.

Key Words: binaries: general — ISM: abundances — stars: individual: XMMSL1 J171900.4–353217 — stars: neutron — X-rays: binaries

1. INTRODUCTION

X-ray binaries are binary systems in which a compact object, either a black hole (BH) or a neutron star (NS), accretes matter from a companion star. When the companion is a low-mass star ($M \lesssim 1{\rm M}_\odot$), the system is known as a low-mass X-ray binary (LMXB). Many LMXBs are transient: they become bright only during outbursts of active accretion, but are more often found in a dim quiescent state.

In quiescence, LMXBs have a low X-ray luminosity of $L_{\rm X} \lesssim^{33}$ erg s^{-1} (e.g., Wijnands et al. 2017). The maximum luminosity that is reached in outburst can vary a lot from source to source, and even from outburst to outburst for a single object. While many LMXBs are bright, with 2–10 keV peak luminosities of $L_{\rm X} \simeq 10^{37} - 10^{39}$ erg s^{-1}, some also exhibit 'mini outbursts' that reach much lower peak luminosities of $L_{\rm X} \simeq 10^{34} - 10^{36}$ erg s^{-1} (e.g., Degenaar

[1]Astronomy and Space Science Department, Faculty of Science, King Abdulaziz University, Kingdom of Saudi Arabia.
[2]Department of Physics, Faculty of Natural and computational Sciences, Debre Tabor University, Ethiopia.
[3]Anton Pannekoek Institute for Astronomy, University of Amsterdam, The Netherlands.
[4]Instituto de Astrofísica de Canarias, Spain.
[5]Departamento de Astrofísica, Universidad de La Laguna, Tenerife, Spain.

& Wijnands 2009; Wijnands & Degenaar 2013; Coti Zelati et al. 2014; Zhang et al. 2019). These are often shorter than regular bright outbursts, although there are also LMXBs that accrete at such a low-luminosity level for extended periods of time (Šimon 2004; Degenaar et al. 2014; Allen et al. 2015; Parikh et al. 2018).

Interestingly, a growing number of systems has been discovered that exhibit maximum outburst luminosities of $L_{\rm X} \simeq 10^{34} - 10^{36}$ erg s^{-1} and seemingly never exhibit brighter outbursts (Sakano et al. 2005; Muno et al. 2005b; Degenaar & Wijnands 2009; Bozzo et al. 2015; Bahramian et al. 2021). These LMXBs belong to the class of very faint X-ray transients (VFXTs; Wijnands et al. 2006). Many of these VFXTs are found near the Galactic center, but this is very likely a selection bias since this region has been regularly surveyed by many X-ray missions. Hence, the brief and dim outbursts of VFXTs are more easily discovered than in other regions of our Galaxy (e.g., Muno et al. 2005b; Sakano et al. 2005; Wijnands et al. 2006; Degenaar et al. 2015).

VFXTs could be intrinsically brighter sources located at large distances (tens of kpc) within the Milky Way, but estimates from thermonuclear bursts could place them nearer[6]. In addition, while inclination effects could possibly make these systems appear fainter than they intrinsically are (e.g., Muno et al. 2005a), this can likely only account for a small fraction of the VFXTs (see King & Wijnands 2006). Many VFXTs are thus expected to be intrinsically faint, i.e. they accrete at low rates. This makes them interesting for a number of scientific reasons. For instance, they probe a little explored mass-accretion regime, hence are valuable for studying accretion physics (e.g., Armas Padilla et al. 2013a; Weng & Zhang 2015; Degenaar et al. 2017). In addition, VFXTs are interesting for testing and improving binary evolution models (e.g. King & Wijnands 2006; Degenaar & Wijnands 2010; Maccarone et al. 2015), and for increasing our understanding of nuclear burning on the surface of accreting NS (e.g., Peng et al. 2007; Degenaar et al. 2010a).

Despite the fact that the number of VFXTs has now grown to a few tens of systems (e.g., Bahramian & Degenaar 2023) and detailed studies of several systems have been performed over the past decade, still much remains to be learned about this source class. For instance, there is no clear picture yet about the distribution of system properties such as the nature of the compact accretor, the type of companion star, and the size of the orbit. Determining whether an LMXB harbors a NS or a BH requires direct measurements of the physical properties of the compact object, such as its mass, or to detect the presence of a solid surface (e.g., through X-ray pulsations or thermonuclear bursts). However, such measurements are often challenging for VFXTs due to their faintness (e.g., making pulsation searches challenging; van den Eijnden et al. 2018) and low accretion rates (e.g., rendering thermonuclear bursts rare; Degenaar et al. 2011).

For some VFXTs, indirect approaches using the ratio between the X-ray and radio or optical/infrared luminosity have been employed to assess the nature of the compact accretor (e.g., Armas Padilla et al. 2011a; Paizis et al. 2011). However, their short outbursts often make it difficult to identify a counterpart for VFXTs at other wavelengths (e.g., Shaw et al. 2020). Furthermore, due to their low accretion rates, not many VXFTs have been detected in the radio band (van den Eijnden et al. 2021) and for finding optical/infrared counterparts additional complications arise from their biased locations in the direction of the Galactic center (i.e., high extinction and crowding; e.g., Bandyopadhyay et al. 2005). Fortunately, an indication of the nature of the accretor can also be obtained by studying the X-ray spectral evolution of VFXTs (Armas Padilla et al. 2011a; Beri et al. 2019; Stoop et al. 2021).

The X-ray properties of LMXBs harboring a NS can be very similar to those containing a BH. However, when comparing their X-ray spectra at low luminosities of $L_{\rm X} \simeq 10^{34} - 10^{36}$ erg s^{-1}, it turns out that confirmed or candidate BH systems have significantly harder spectra than confirmed NSs. In addition, the BH spectra show a strong softening when the X-ray lumninosity evolves below $\simeq 10^{34}$ erg s^{-1}, while NSs start to show clear softening already at higher X-ray luminosities of $L_{\rm X} \simeq 10^{36}$ erg s^{-1} (e.g., Wijnands et al. 2015; Parikh et al. 2017).

Over the last few years, detailed studies have been performed for a growing number of VFXTs and the general conclusion is that due to low statistics on their X-ray spectra, such systems can be satisfactorily described with a simple power-law model, with a soft (black body) component only being distinguishable when high quality (i.e. many counts) data are

[6]Thermonuclear burst, or type-I bursts, are brief (seconds to hours) flashes of X-ray emission caused by unstable nuclear burning of gas accreted onto a neutron star. These explosions are thought to reach the Eddington limit and can therefore be employed to derive a distance to the bursting LMXB (e.g., Kuulkers et al. 2003). They are exhibited by many VFXTs, which place them at distances of only several kpc and they must thus have low intrinsic luminosities (e.g., Cornelisse et al. 2002; Lutovinov et al. 2005; Degenaar et al. 2010a; Bozzo et al. 2015; Keek et al. 2017)

TABLE 1

LOG OF *SWIFT*/XRT OBSERVATIONS

Obs	Observation ID	Date and start time (UT)	Exposure time (ks)	Net count rate (ct s^{-1})
1	00031719001	2010 May 11 16:56	2.0	0.4
2	00031719002	2010 May 31 12:23	1.0	0.1
3	00031719003	2010 June 14 11:44	1.2	0.2
4	00031719004	2010 June 29 06:42	1.7	0.7
5	00031719005	2010 July 13 09:29	1.0	<0.008
6	00031719006	2010 August 20 13:00	2.5	0.3
7	00031719007	2010 October 15 02:10	1.3	<0.002

available (e.g., Armas Padilla et al. 2011a). However, irrespective of what model is fitted to the spectra, VFXTs also become softer with decreasing X-ray luminosity. Their X-ray spectral evolution during an outburst can thus be used as a diagnostic for the nature of the compact accretor.

1.1. *Discovery of XMMSL1 J171900.4–353217*

XMMSL1 J171900.4–353217 was discovered as an X-ray transient in *XMM-Newton* slew data obtained on 2010 March 10 (Read et al. 2010a). The source location was in FOV of *INTEGRAL* observations performed around the same time, but it was not detected (20–40 keV; Bozzo et al. 2010). Markwardt et al. (2010) pointed out that XMMSL1 J171900.4–353217 was likely associated to a faint transient source, XTE J1719–356, detected in *RXTE*/PCA scans of the Galactic bulge since 2010 March.

Observations performed with the X-Ray Telescope (XRT; Burrows et al. 2005) onboard the *Neil Gehrels Swift Observatory* (*Swift*; Gehrels et al. 2004) in 2010 May, showed that the source was still active, i.e. two months after the initial discovery (Read et al. 2010b). Armas Padilla et al. (2010b,a) reported on further *Swift*/XRT observations, performed in 2010 May and June, which showed that the source remained active in soft X-rays, albeit with varying flux. While *Swift*/XRT did no longer detect the source in 2010 July, suggesting it had returned to quiescence (Armas Padilla et al. 2010c), *INTEGRAL* serendipitously detected the source in hard X-rays in August 2010 (20–40 keV; Ishibashi et al. 2010). It was also detected again in soft X-rays with *Swift*/XRT around that time (Pavan et al. 2010). Nothing more was reported on the source after this.

In this work we investigate the nature of the compact accretor in the VFXT XMMSL1 J171900.4–353217 by studying its X-ray spectral evolution as seen with *Swift*/XRT.

2. OBSERVATIONS AND DATA ANALYSIS

XMMSL1 J171900.4–353217 was observed over a 157 days time-span with *Swift*, between 2010 May 11 and October 15 (see Table 1). Seven pointed observations were carried out during this time and we investigate the data collected using the XRT.

2.1. *Description of the Data Reduction*

All XRT data were collected in photon counting (PC) mode. We reduced the data and obtained science products using the HEASOFT software package (v. 6.26). We cleaned the data by running the XRTPIPELINE task in which standard event grades of 0–12 were selected. For every observation, images, count rates and spectra were obtained with the XSELECT (v.2.4) package. We extracted the source events using a circular region with a radius of 52 arcseconds. The background emission was averaged over three circular regions of similar size that were placed on nearby, source-free parts of the image.

The source was detected in 5 of the 7 observations (see Table 1) and for these we extracted spectra. Using GRPPHA, three spectra were grouped to have 10 counts per energy bin, one was grouped to 20 counts per bin (observation ID 00031719004, when the source was brightest), and one to 5 counts per bin (observation ID 00031719002 when the source was faintest).

The spectra were corrected for the fractional exposure loss due to bad columns on the CCD. For this, we created exposure maps with the XRTEXPOMAP task, which were then used as an input to generate the ancillary response files (arf) with the XRTMKARF task. We acquired the response matrix file (rmf) from the HEASARC calibration database (v.12).

2.2. *Pile-Up*

Observation 00031719004 has the highest count rate (0.7 ct s^{-1}) and is affected by pile-up. We tested

this following the steps outlined in the dedicated XRT analysis thread[7]. Following these guidelines, we found that five pixels had to be excluded in the bright core to mitigate the effect of pile-up. The remaining six observations have < 0.5 ct s^{-1} and are not affected by pile-up (see Table 1).

3. RESULTS

3.1. *X-ray Spectral Fitting*

To fit the X-ray spectra, we used XSPEC[8] (v.12.10.1; Arnaud 1996). Given the low count rates (Table 1), we used simple power law (PEGPWRLW) and black body (BBODYRAD) models to describe the data. For both models, we took into account interstellar extinction by including the TBABS model, and used C-statistics due to low data counts. For this absorption model we used abundances set to those of Wilms et al. (2000) and the cross-sections from Verner et al. (1996). Both models yielded the same quality of fit, so that we cannot statistically prefer one model over the other. However, in order to use the Wijnands et al. (2015) method to probe the nature of the compact accretor, we need to use the power-law model. Therefore, we here report on the results from fitting the absorbed power-law model, but we include the results for the absorbed blackbody fits in the Appendix, for completeness.

We also briefly explored whether the spectrum could be composed of two emission components, such as has been seen for VFXTs that have high-quality data available (e.g., Armas Padilla et al. 2011a, 2013a; Degenaar et al. 2017). For this we used the observation with the highest flux (observation ID 00031719004). We first fitted this to an absorbed power law, then added a black body component and re-fitted. This resulted in similar fit parameters as for the single absorbed power-law model. The two-component model adequately fits the spectra by eye, but the extra thermal component is not statistically required (F-test probability > 0.99). It is likely that the low number of counts in the spectrum does not allow us to detect a second component, even if it is present. We therefore did not test this for the other observations, since these have even lower count rates. We conclude that a single-component model can adequately fit the *Swift* spectra.

Using the convolution model CFLUX within XSPEC, and setting the energy range to 0.5 to 10 keV, we determined both the absorbed ($F_{\rm X,abs}$) and unabsorbed fluxes ($F_{\rm X,unabs}$). The results are listed in Table 2. In Figure 1 we show the light curve

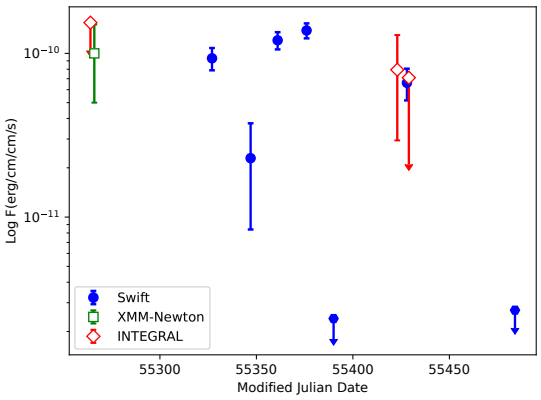

Fig. 1. Evolution of 0.5 – 10 keV unabsorbed flux of XMMSL1 J171900.4–353217, inferred from our spectral analysis of the *Swift*/XRT data (blue filled circles). To show the full outburst, we include points reported in the literature from *INTEGRAL* (red open diamonds) and *XMM-Newton* (green open square), which were converted to 0.5–10 keV for this purpose (see § 3.3 and Table 3). The color figure can be viewed online.

constructed from the unabsorbed fluxes. From the seven XRT observations, the highest unabsorbed flux we measure is $F_{\rm X,unabs} = 13.8 \times 10^{-11}$ erg cm^{-2} s^{-1} in observation 00031719004 (see Figure 1 and Table 2). In Figure 2 we show the *Swift*/XRT spectrum of this observation.

3.2. *Flux Upper Limits for XRT Non-Detections*

In observations 00031719005 and 00031719007 the source was not detected with the XRT. For these observations, we determined the net counts detected at the source position with XSELECT (using similar source and background extraction regions as for the other observations; see § 2.1). For observation 00031719005 (1 ks) we detect 4 counts at the source position and 1 count averaged over the background regions. For observation 00031719007 (1.3 ks), we measure 6 counts for the source and none for the background. Accounting for small number statistics using the tables of Gehrels (1986), we determine a 95% upper limit on the detected net source counts of 7.75 and 11.84 for observations 00031719005 and 00031719007, respectively. Dividing by the exposure times then gives 95% confidence count rate upper limits of $< 7.9 \times 10^{-3}$ ct s^{-1} (00031719005) and $< 9.1 \times 10^{-3}$ ct s^{-1} (00031719007).

To estimate flux upper limits for the non-detections, we used WEBPIMMS[9] to convert the count

[7] https://www.swift.ac.uk/analysis/xrt/pileup.php.
[8] https://heasarc.gsfc.nasa.gov/xanadu/xspec/.
[9] https://heasarc.gsfc.nasa.gov/cgi-bin/Tools/w3pimms/w3pimms.pl.

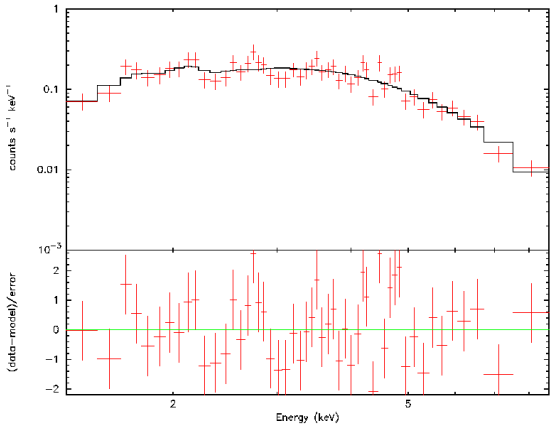

Fig. 2. An X-ray spectrum of XMMSL1 J171900.4–353217 detected with *Swift*/XRT. Upper panel: shows the brightest observation, 00031719004, fitted with an absorbed power law model. Bottom panel: shows the corresponding fit residuals in units of σ. The color figure can be viewed online.

rate upper limits, assuming an absorbed power-law model with a photon index of $\Gamma = 2.49$ and a hydrogen column density of $N_{\rm H} = 5.81 \times 10^{22}$ cm^{-2}. We choose those values because these are the ones we obtained for the observation with the lowest flux (observation 00031719002).

3.3. *X-ray Spectral Evolution*

The distance to XMMSL1 J171900.4–353217 is unknown. We therefore took three different values of 4, 8 and 12 kpc, to calculate the 0.5–10 keV luminosity from the unabsorbed flux. These results are included in Table 2. In Figure 3 we plot the evolution of the power-law index versus luminosity of XMMSL1 J171900.4–353217 along with the sample of NS (red filled circles) and BH (black crosses) LMXBs of Wijnands et al. (2015). We then overplot XMMSL1 J171900.4–353217 as blue open diamonds for different distances of 4, 8, and 12 kpc in subpanels a, b, and c, respectively.

We find that for all distances, our data points fall among the NS sample, but above the BH track. This would suggest that the source is either a proximate ($\lesssim 4$ kpc) BH, or a NS located around or beyond 4 kpc. Considering the high $N_{\rm H}$ towards the source, both as inferred from our X-ray spectral fitting ($N_{\rm H} \simeq 5 \times 10^{22}$ cm^{-2}) and from Galactic extinction maps ($N_{\rm H} \simeq 1 \times 10^{22}$ cm^{-2}; Bekhti et al. (2016)), we consider a larger distance more likely, and hence tentatively favor a NS nature. However,

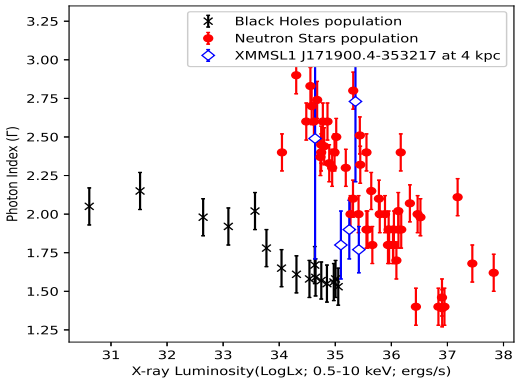

(a)

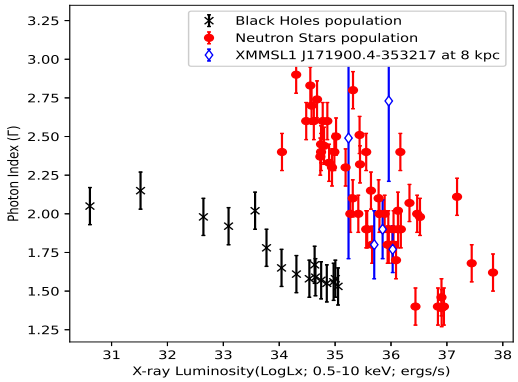

(b)

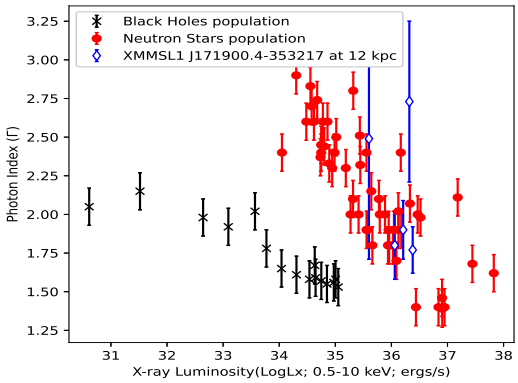

(c)

Fig. 3. Power law index versus X-ray luminosity in the 0.5–10 keV range for XMMSL1 J171900.4–353217 as well as a sample of NS (red circles) and BH (grey crosses) LMXBs (from Wijnands et al. 2015). For XMMSL1 J171900.4–353217 we used three different distances of 4 kpc (panel a), 8 kpc (panel b) and 12 kpc (panel c). The color figure can be viewed online.

TABLE 2

RESULTS FROM ANALYSING THE *SWIFT*/XRT SPECTRA

Obs	$N_{\rm H}$ (10^{22}cm^{-2})	Γ	$F_{\rm X,abs}$ (10^{-11} erg cm^{-2}s^{-1})	$F_{\rm X,unabs}$	$L_{\rm X}$ 4 kpc	$L_{\rm X}$ 8 kpc (10^{35} erg s^{-1})	$L_{\rm X}$ 12 kpc
1	$5.45^{+0.64}_{-0.61}$	1.90 ± 0.19	4.17 ± 0.19	$9.33^{+1.63}_{-1.20}$	$1.78^{+0.32}_{-0.23}$	$7.14^{+1.25}_{-0.92}$	$16.07^{+2.81}_{-5.07}$
2	$5.81^{+2.35}_{-1.98}$	$2.49^{+0.78}_{-0.70}$	$0.57^{+0.12}_{-0.09}$	$2.29^{+4.02}_{-1.03}$	$0.44^{+0.76}_{-0.20}$	$1.73^{+3.08}_{-0.79}$	$3.94^{+6.93}_{-1.77}$
3	$7.85^{+1.87}_{-1.77}$	2.73 ± 0.52	$2.04^{+0.25}_{-0.22}$	$12.02^{+13.09}_{-5.26}$	$2.30^{+2.50}_{-1.01}$	$9.20^{+10.02}_{-4.02}$	$20.7^{+22.55}_{-9.06}$
4	$4.60^{+0.47}_{-0.45}$	1.77 ± 0.15	$7.01^{+0.40}_{-0.25}$	$13.80^{+1.69}_{-1.21}$	$2.64^{+0.32}_{-0.23}$	$10.75^{+1.29}_{-0.93}$	$23.77^{+2.91}_{-2.09}$
5	5.81 fix	2.49 fix	< 0.06	< 0.24	< 0.05	< 0.19	< 0.42
6	$6.67^{+0.89}_{-0.86}$	1.80 ± 0.22	2.95 ± 0.20	$6.61^{+1.33}_{-0.86}$	$1.26^{+0.26}_{-0.16}$	$5.06^{+1.02}_{-0.66}$	$11.38^{+2.29}_{-1.48}$
7	5.81 fix	2.49 fix	< 0.07	< 0.27	< 0.06	< 0.21	< 0.47

TABLE 3

OTHER REPORTED X-RAY FLUX MEASUREMENTS

Observatory (detector)	Date	Reported Brightness (various formats)	$F_{\rm X,abs}$[a]	$F_{\rm X,unabs}$[a]	Reference[b]
			(10^{-11} erg cm^{-2}s^{-1})		
XMM-Newton (PN)	2010 March 10	4.5 c s^{-1} (0.2–10 keV)	4.5	10.2	1
INTEGRAL (IBIS)	2010 March 09	<6 mCrab (20–40 keV)	< 6.82	< 15.40	2
INTEGRAL (IBIS)	2010 August 14	3.0×10^{-11} erg cm^{-2} s^{-1} (20–40 keV)	3.55	7.94	3
INTEGRAL (IBIS)	2010 August 20	$<2.7\times10^{-11}$ erg cm^{-2} s^{-1}(20−40 keV)	<3.2	<7.1	4

[a]The quoted count rates were converted to 0.5–10 keV fluxes using WEBPIMMS and assuming a power-law spectral model. For the first two table entries we used $N_{\rm H} = 5.45 \times 10^{22}$ cm^{-2} and $\Gamma = 1.90$, for the last two $N_{\rm H} = 6.67 \times 10^{22}$ cm^{-2} and $\Gamma = 1.80$. These parameter values match those found from our spectral fitting of *Swift*/XRT data obtained around that time (see Table 2).

[b]References: 1=Read et al. (2010a), 2=Bozzo et al. (2010), 3=Ishibashi et al. (2010), 4=Pavan et al. (2010).

the reader should bear in mind that a BH nature cannot be excluded.

3.4. *Time-Averaged Accretion Rate*

We continue to calculate the time-averaged accretion rate for XMMSL1 J171900.4–353217, since this is an interesting parameter to understand the possible evolution paths of VFXTs (King & Wijnands 2006). We initially assume that the source contains a NS primary and then calculate the mean outburst accretion rate, $\langle \dot{M}_{\rm ob} \rangle$, from the mean unabsorbed flux measured during the outburst. For this purpose, we add the *INTEGRAL* and *XMM-Newton* fluxes reported in the literature to our results obtained with *Swift*.

We used WEBPIMMS to convert reported instrument count rates or 20–40 keV fluxes to unabsorbed 0.5–10 keV fluxes. All information used for these conversions is listed in Table 3. We assumed an absorbed power-law spectral shape. For the *XMM-Newton* and first *INTEGRAL* observations, both performed in March 2010, we used $N_{\rm H} = 5.45 \times 10^{22}$ cm^{-2} and $\Gamma = 1.90$, which are the values we obtained from spectral fitting for the *Swift*/XRT observations performed closest in time (observation 00000031719001; see Tables 1–3). For the other two *INTEGRAL* observations, both performed in 2010 August, we assumed $N_{\rm H} = 6.67 \times 10^{22}$ cm^{-2} and $\Gamma = 1.80$ as found from fitting the *Swift*/XRT spectrum obtained closest in time (observation 00000031719006).

The resulting 0.5–10 keV flux light curve is shown in Figure 1. From all these data points we determine a mean 0.5–10 keV outburst flux of 8.9×10^{-11} erg cm^{-2} s^{-1}. Based on this, we estimate the 0.1–100 keV accretion luminosity by assuming a bolometric correction factor of 3 (following in't Zand et al. 2007). The mass transfer rate of the outburst was then computed using the equation $\langle \dot{M}_{\rm ob} \rangle = R_{\rm Ns} L_{\rm acc}/{\rm G}M_{\rm Ns}$, where ${\rm G} = 6.67\times10^{-8}$ cm^{3}g^{-1}s^{-2} is the gravitational constant. Assuming $R_{\rm Ns} = 1.1 \times 10^6$ cm = 11 km and $M_{\rm Ns} = 1.5$ M$_\odot$, the outburst mass accretion rate we obtain is $\langle \dot{M}_{\rm ob} \rangle \simeq 1.7 \times 10^{-10}$ M$_\odot$ yr^{-1}.

We can next estimate the mean long-term averaged accretion rate using $\langle \dot{M}_{\rm long} \rangle = \langle \dot{M}_{\rm ob} \rangle \times t_{\rm ob}/t_{\rm rec}$, where $t_{\rm ob}$ is the outburst duration, $t_{\rm rec}$ is the system's recurrence time, and the ratio of the two represents its duty cycle. Neither the onset nor the fad-

ing of the outburst into quiescence have been observed for XMMSL1 J171900.4–353217, so the total outburst duration is unconstrained.[10] If we assume that the source was continuously active (i.e., only occasionally dropping to non-detectable flux levels) between its first and last detection on 2010 March 9 and 2010 August 20, the minimum outburst duration is 164 days. Since this was the first and only outburst ever observed for the source, its recurrence time is also unconstrained. For the present purpose we assume a duty cycle of 1–10% based on long-term X-ray monitoring of VFXTs in the Galactic center (Degenaar & Wijnands 2009, 2010). This would imply an outburst recurrence time of 4.5–45 yr for XMMSL1 J171900.4–353217, and yields a mean long-term accretion rate of $\langle \dot{M}_{\rm long} \rangle \simeq 0.17 - 1.7 \times 10^{-11}$ M$_\odot$ yr^{-1}.

We note that if the source harbors a black hole accretor, the above estimates for the (long-term) mass accretion rate would be a factor $\simeq 10$ lower due to the mass difference between neutron stars and black holes.

4. DISCUSSION

We report on the properties of the discovery outburst of the X-ray transient XMMSL1 J171900.4–353217, which lasted more than 164 days in 2010. We studied the X-ray spectral evolution of the source using the Swift/XRT data and used the method of Wijnands et al. (2015) to investigate the nature of the accreting object. Based on the evolution of its power-law index with 0.5–10 keV luminosity, we conclude that XMMSL1 J171900.4–353217 is most likely a NS LMXB located at several kpc.

Adding to our *Swift*/XRT results flux measurements reported in the literature (from *XMM-Newton* and *INTEGRAL* observations), we constructed the light curve of the 2010 outburst (see Figure 1). Over the 5.5 months that the source was observed to be active, the maximum 0.5–10 keV unabsorbed flux detected with *Swift*/XRT was $F_{\rm X,unabs}^{\rm peak} = 13.8 \times 10^{-11}$ erg cm^{-2} s^{-1}. For a distance of 8 kpc, this peak flux translates into a luminosity of $L_{\rm X}^{\rm peak} \simeq 1.1 \times 10^{36}$ erg s^{-1}. This classifies XMMSL1 J171900.4–353217 as a VFXT.[11]

We furthermore estimated a mean unabsorbed flux along the observations of $F_{\rm X}^{\rm avg} \simeq 8.9 \times 10^{-11}$ erg cm^{-2} s^{-1}. For a distance of 8 kpc, this translates into a luminosity of $L_{\rm X}^{\rm avg} \simeq 6.8 \times 10^{35}$ erg s^{-1}. We used this information to estimate the average accretion rate along the outburst as $< \dot{M}_{\rm ob} > \simeq 1.7 \times 10^{-10}$ M$_\odot$ yr^{-1}. If the source has a duty cycle of 1–10%, which is not uncommon for LMXBs and VFXTs (Degenaar & Wijnands 2010), we can then estimate a long-term average accretion rate of $< \dot{M}_{\rm long} > \simeq 0.17 - 1.7 \times 10^{-11}$ M$_\odot$ yr^{-1}. This is in the same range as inferred for the VFXTs in the Galactic Center (Degenaar & Wijnands 2009, 2010). Very low long-term average accretion rates can only be explained if these systems have hydrogen poor companions or are born with low companion masses (King & Wijnands 2006). However, the current (faint) accretion activity may not necessarily be representative for the long-term behavior of these systems (Wijnands et al. 2013).

In the past years, several NS LMXBs with similarly low outburst luminosities (hence accretion rates) as XMMSL1 J171900.4–353217 were uncovered to harbor accreting millisecond X-ray pulsars (AMXPs). Examples are IGR J17062–6143 (Strohmayer & Keek 2017), IGR J17591–2342 (Sanna et al. 2018b), IGR J17379–3747 (Sanna et al. 2018a) and IGR J17494–3030 (Ng et al. 2020). All were previously known VXFTs that were observed during (new) outbursts with *NICER*, which detected the X-ray pulsations. Given the similar X-ray spectral properties of XMMSL1 J171900.4–353217 with those sources, we hypothesize that it may also harbor a millisecond X-ray pulsar. Indeed, one of the sources mentioned above was proposed to be a NS based on the same method as we employ here (Armas Padilla et al. 2013b) and later found to be an AMXP (Ng et al. 2020). Therefore, should XMMSL1 J171900.4–353217 enter a new accretion outburst in the future, we encourage X-ray observations (in particular with *NICER*) to search for pulsations that would confirm the NS nature of this source, and allow for a measurement of its orbital period. In case a new outburst occurs, we also encourage dense monitoring of the outburst decay (in particular with *Swift*), since this can also provide an indication of the orbital period and nature of the compact accretor (e.g., Armas Padilla et al. 2011a; Heinke et al. 2015; Stoop et al. 2021).

[10] We note that in the *RXTE*/PCA bulge scans the possibly associated transient XTE J1719–356 seems to be detected on and off between 2010 March and September, but not thereafter. The *RXTE* data therefore does not provide additional constraints on the outburst duration. See `https://asd.gsfc.nasa.gov/Craig.Markwardt/galscan/html/XTE_J1719-356.html`.

[11] We note that Wijnands et al. (2006) uses the 2–10 keV band to define luminosity classes whereas we here use 0.5–10 keV. However, since the 0.5–10 keV luminosity is higher than the 2–10 keV luminosity, our conclusion that XMMSL1 J171900.4–353217 falls in the regime of VFXTs still holds.

TABLE 4

RESULTS FROM XRT SPECTRAL ANALYSIS USING A BLACK-BODY MODEL. X-RAY FLUXES AND LUMINOSITIES ARE GIVEN IN THE 0.5–10 KEV ENERGY BAND

Obs	$N_{\rm H}$ (10^{22} cm^{-2})	kT (keV)	$F_{\rm X_{abs}}$ (10^{-11} erg cm^{-2}s^{-1})	$F_{\rm X_{unabs}}$	$L_{\rm X}$ 4 kpc	$L_{\rm X}$ 8 kpc (10^{35} erg s^{-1})	$L_{\rm X}$ 12 kpc
1	2.23 ± 0.40	$1.32^{+0.08}_{-0.07}$	$3.71^{+0.18}_{-0.16}$	4.47 ± 0.20	$0.85^{+0.04}_{-0.03}$	$3.42^{+0.16}_{-0.18}$	$7.70^{+0.36}_{-0.35}$
2	$2.29^{+1.56}_{-1.29}$	$1.06^{+0.24}_{-0.19}$	$0.50^{+0.10}_{-0.08}$	$0.65^{+0.12}_{-0.11}$	$0.12^{+0.03}_{-0.02}$	0.51 ± 0.09	$1.12^{+0.21}_{-0.19}$
3	$3.38^{+1.26}_{-1.19}$	$1.01^{+0.13}_{-0.11}$	$1.74^{+0.21}_{-0.16}$	$2.51^{+6.61}_{-1.72}$	$0.48^{+1.26}_{-0.33}$	$1.92^{+5.06}_{-1.32}$	$4.32^{+11.39}_{-2.96}$
4	$1.69^{+0.31}_{-0.30}$	$1.34^{+0.07}_{-0.06}$	$6.17^{+0.29}_{-0.28}$	$7.24^{+0.35}_{-0.32}$	$1.38^{+0.07}_{-0.06}$	$5.54^{+0.27}_{-0.24}$	$12.47^{+0.6}_{-0.55}$
5	2.29 fix	1.06 fix	< 0.05	< 0.07	< 0.02	< 0.06	< 0.13
6	$2.96^{+0.60}_{-0.57}$	$1.41^{+0.10}_{-0.09}$	2.63 ± 0.18	3.24 ± 0.15	0.62 ± 0.03	$2.48^{+0.12}_{-0.11}$	5.58 ± 0.26
7	2.29 fix	1.06 fix	< 0.06	< 0.08	< 0.02	< 0.07	< 0.15

Quoted errors reflect 1-σ confidence intervals.

OA is grateful to Sera Markoff and the Anton Pannekoek Institute for organizing and hosting the Advanced Theoretical Astrophysics summer school in 2019, which fostered the collaboration that led to this work. ND was partly supported by a Vidi grant awarded by the Netherlands organization for scientific research (NWO). This work made use of data supplied by the UK *Swift* Science Data Centre at the University of Leicester. M. A. P. acknowledges support from the Spanish ministry of science under Grant PID2020–120323GB-I00. M. A. P. acknowledges support from the Consejeria de Economia, Conocimiento y Empleo del Gobierno de Canarias and the European Regional Development Fund under grant ProID2021010132.

APPENDIX

A1. BLACK-BODY SPECTRAL FITTING RESULTS

For completeness we here report on the results of fitting the *Swift*/XRT spectra of XMMSL1 J171900.4–353217 with an absorbed black body model. For the upper limit calculation of the two XRT non-detections, we now used kT = 1.06 keV and $N_H = 2.29 \times 10^{22}$ cm^{-2}. These are the values we obtained for the observation with the lowest flux (observation ID 00031719002). All results are listed in Table 4.

REFERENCES

Allen, J. L., Linares, M., Homan, J., & Chakrabarty, D. 2015, ApJ, 801, 10, https://doi.org/10.1088/0004-637X/801/1/10

Armas Padilla, M., Degenaar, N., Kaur, R., Wijnands, R., & Yang, Y. 2010a, Atel, 2738, 1

Armas Padilla, M., Degenaar, N., Patruno, A., et al. 2011a, MNRAS, 417, 659, https://doi.org/10.1111/j.1365-2966.2011.19308.x

Armas Padilla, M., Degenaar, N., & Wijnands, R. 2013a, MNRAS, 434, 1586, https://doi.org/10.1093/mnras/stt1114

Armas Padilla, M., Degenaar, N., Yang, Y., Patruno, A., & Wijnands, R. 2010b, Atel, 2656, 1

Armas Padilla, M., Kaur, R., Degenaar, N., et al. 2010c, Atel, 2722, 1

Armas Padilla, M., Wijnands, R., & Degenaar, N. 2013b, MNRAS, 436, 89, https://doi.org/10.1093/mnrasl/slt119

Arnaud, K. A. 1996, ASPC 101, XSPEC: The First Ten Years, Astronomical Data Analysis Software and Systems, 17, 1

Bahramian, A. & Degenaar, N. 2023, in Handbook of X-ray and Gamma-ray Astrophysics, ed. C. Bambi and A. Santangelo, (Singapore:Springer), 120, https://doi.org/10.1007/978-981-19-6960-7

Bahramian, A., Heinke, C. O., Kennea, J. A., et al. 2021, MNRAS, 501, 2790, https://doi.org/10.1093/mnras/staa3868

Bandyopadhyay, R. M., Miller-Jones, J. C. A., Blundell, K. M., et al. 2005, MNRAS, 364, 1195, https://doi.org/10.1111/j.1365-2966.2005.09607.x

Bekhti, N. B., Flöer, L., Keller, R., et al. 2016, A&A, 594, 116, https://doi.org/10.1052/0004-6361/201629178

Beri, A., Altamirano, D., Wijnands, R., Degenaar, N., Parikh, A. S., & Yamaoka, K. 2019, MNRAS, 486, 1620, https://doi.org/10.1093,mnras/stz938

Bozzo, E., Romano, P., Falanga, M., Ferrigno, C., Papitto, A., & Krimm, H. A. 2015, A&A, 579, 56, https://doi.org/10.1051/0004-6361/201526150

Bozzo, E., Weidenspointner, G., Kuulkers, E., Terrier, R., & Carmona, P. K. A. 2010, Atel, 2616, 1

Burrows, D. N., Hill, J. E., Nousek, J. A., et al. 2005, SSRv, 120, 165, https://doi.org/10.1007/s11214-005-5097-2

Cornelisse, R., Verbunt, F., in 't Zand, J., et al. 2002, A&A, 392, 885, https://doi.org/10.1051/0004-6361:20020707

Coti Zelati, F., Campana, S., D'Avanzo, P., & Melandri, A. 2014, MNRAS, 438, 2634, https://doi.org/10.1093/mnras/stt2384

Degenaar, N., Jonker, P., Torres, M., et al. 2010a, MNRAS, 404, 1591, https://doi.org/10.1111/j.1365-2966.2010.16388.x

Degenaar, N., Pinto, C., Miller, J. M., et al. 2017, MNRAS, 464, 398, https://doi.org/10.1093/mnras/stw2355

Degenaar, N. & Wijnands, R. 2009, A&A, 495, 547, https://doi.org/10.1051/0004-6361:200810654

_____. 2010, A&A, 524, 69, https://doi.org/10.1051/0004-6361/201015322

Degenaar, N., Wijnands, R., & Kaur, R. 2011, MNRAS, 414, 104, https://doi.org/10.1111/j.1745-3933.2011.01066.x

Degenaar, N., Wijnands, R., Miller, J. M., et al. 2015, JHEAp, 7, 137, https://doi.org/10.1016/j.jheap.2015.03.005

Degenaar, N., Wijnands, R., Reynolds, M. T., et al. 2014, ApJ, 792, 109, https://doi.org/10.1088/0004-637X/792/2/109

Gehrels, N. 1986, ApJ, 303, 336, https://doi.org/10.1086/164079

Gehrels, N., Chincarini, G., Giommi, P., et al. 2004, ApJ, 611, 1005, https://doi.org/10.1086/422091

Heinke, C. O., Bahramian, A., Degenaar, N., & Wijnands, R. 2015, MNRAS, 447, 3034, https://doi.org/10.1093/mnras/stu2652

in't Zand, J. J. M., Jonker, P. G., & Markwardt, C. B. 2007, A&A, 465, 953, https://doi.org/10.1051/0004-6361:20066678

Ishibashi, W., Bozzo, E., Terrier, R., et al. 2010, Atel, 2803, 1

Keek, L., Iwakiri, W., Serino, M., et al. 2017, ApJ, 836, 111, https://doi.org/10.3847/1538-4357/836/1/111

King, A. R. & Wijnands, R. 2006, MNRAS, 366, 31, https://doi.org/10.1111/j.1745-3933.2005.00126.x

Kuulkers, E., den Hartog, P. R., in't Zand, J. J. M., et al. 2003, A&A, 399, 663, https://doi.org/10.1051/0004-6361:20021781

Lutovinov, A., Revnivtsev, M., Molkov, S., & Sunyaev, R. 2005, A&A, 430, 997, https://doi.org/10.1051/0004-6361:20041677

Maccarone, T. J., Wijnands, R. A. M., Degenaar, N., et al. 2015, arXiv:1501.02769, https://doi.org/10.48550/arXiv.1501.02769

Markwardt, C. B., Strohmayer, T. E., & Swank, J. H. 2010, Atel, 2615, 1

Muno, M. P., Lu, J. R., Baganoff, F. K., et al. 2005a, ApJ, 633, 228, https://doi.org/10.1086/444586

Muno, M. P., Pfahl, E., Baganoff, F. K., et al. 2005b, ApJ, 622, 113, https://doi.org/10.1086/429721

Ng, M., Ray, P. S., Strohmayer, T. E., et al. 2020, Atel, 14124, 1

Paizis, A., Nowak, M. A., Wilms, J., et al. 2011, ApJ, 738, 183, https://doi.org/10.1088/0004-637X/738/2/183

Parikh, A. S., Wijnands, R., Degenaar, N., & Altamirano, D. 2018, Atel, 11869, 1

Parikh, A. S., Wijnands, R., Degenaar, N., et al. 2017, MNRAS, 468, 3979, https://doi.org/10.1093/mnras/stx747

Pavan, L., Terrier, R., Bozzo, E., et al. 2010, Atel, 2807, 1

Peng, F., Brown, E. F., & Truran, J. W. 2007, ApJ, 654, 1022, https://doi.org/10.1086/509628

Read, A. M., Saxton, R. D., & Esquej, P. 2010a, Atel, 2607, 1

Read, A. M., Saxton, R. D., Esquej, P., & Evans, P. A. 2010b, Atel, 2627, 1

Sakano, M., Warwick, R. S., Decourchelle, A., & Wang, Q. D. 2005, MNRAS, 357, 1211, https://doi.org/10.1111/j.1365-2966.2005.08717.x

Sanna, A., Bozzo, E., Papitto, A., et al. 2018a, A&A, 616, 17, https://doi.org/10.1051/0004-6361/201833205

Sanna, A., Ferrigno, C., Ray, P. S., et al. 2018b, A&A, 617, 8, https://doi.org/10.1051/0004-6361/201834160

Shaw, A. W., Heinke, C. O., Maccarone, T. J., et al. 2020, MNRAS, 492, 4344, https://doi.org/10.1093/mnras/staa105

Šimon, V. 2004, A&A, 418, 617, https://doi.org/10.1051&0004-6361:20040037

Stoop, M., van den Eijnden, J., Degenaar, N., et al. 2021, MNRAS, 507, 330, https://doi.org/10.1093/mnras/stab2127

Strohmayer, T. & Keek, L. 2017, ApJ, 836, 23 , https://doi.org/10.3847/2041-8213/aa5e51

van den Eijnden, J., Degenaar, N., Pinto, C., et al. 2018, MNRAS, 475, 2027, https://doi.org/10.1093/mnras/stx3224

van den Eijnden, J., Degenaar, N., Russell, T. D., et al. 2021, MNRAS, 507, 3899, https://doi.org/10.1093/mnras/stab1995

Verner, D. A., Ferland, G. J., Korista, K. T., & Yakovlev, D. G. 1996, ApJ, 465, 487, https://doi.org/10.1086/177435

Weng, S.-S. & Zhang, S.-N. 2015, MNRAS, 447, 486, https://doi.org/10.1093/mnras/stu2610

Wijnands, R. & Degenaar, N. 2013, MNRAS, 434, 1599, https://doi.org/10.1093/mnras/stt1119

Wijnands, R., Degenaar, N., Padilla, M. A., et al. 2015, MNRAS, 454, 1371, https://doi.org/10.1093/mnras/stv1974

Wijnands, R., Degenaar, N., & Page, D. 2013, MNRAS, 432, 2366, https://doi.org/10.1093/mnras/stt599

_____. 2017, JApA, 38, 49, https://doi.org/10.1007/s12036-017-0466-5

Wijnands, R., in't Zand, J. J. M., Rupen, M., et al. 2006, A&A, 449, 1117, https://doi.org/10.1051/0004-6361:20054129
Wilms, J., Allen, A., & McCray, R. 2000, ApJ, 542, 914, https://doi.org/10.1086/317016
Zhang, G. B., Bernardini, F., Russell, D. M., et al. 2019, ApJ, 876, 5, https://doi.org/10.3847/1538-4357/ab12dd

Osman Ahmed: Astronomy and Space Science Department, Faculty of Science, King Abdulaziz University, P.O. Box 80203, Jeddah 21589, Kingdom of Saudi Arabia.
Osman Ahmed: Department of Physics, Faculty of Natural and computational Sciences, Debre Tabor University, P.O. Box 272, South Gondar, Ethiopia.
Nathalie Degenaar and Rudy Wijnands: Anton Pannekoek Institute for Astronomy, University of Amsterdam, Science Park 904, 1098 XH, Amsterdam, The Netherlands.
Montserrat Armas Padilla: Instituto de Astrofísica de Canarias, 38205, San Cristobal de La Laguna, Spain.
Montserrat Armas Padilla: Departamento de Astrofísica, Universidad de La Laguna, E-38206 La Laguna, Tenerife, Spain.